Biochemical and Biophysical Research Communications 518 (2019) 719–725

Contents lists available at ScienceDirect

Biochemical and Biophysical Research Communications

journal homepage: www.elsevier.com/locate/ybbrc

Rapeseed calcium-dependent protein kinase CPK6L modulates reactive oxygen species and cell death through interacting and phosphorylating RBOHD

Gengyu Pan, Hanfeng Zhang, Bingyou Chen, Shidong Gao, Bo Yang, Yuan-Qing Jiang*

State Key Laboratory of Soil Erosion and Dryland Farming on the Loess Plateau, College of Life Sciences, Northwest A & F University, Yangling, Shaanxi, 712100, China

ARTICLE INFO

Article history:
Received 22 August 2019
Accepted 23 August 2019
Available online 28 August 2019

Keywords:
Rapeseed
Calcium-dependent protein kinase
Respiratory burst oxidase homolog
Reactive oxygen species
Cell death

ABSTRACT

Reactive oxygen species (ROS) play important roles in plant growth, development, responses to abiotic and biotic stresses. Hypersensitive response (HR)-like cell death is often associated with excess ROS. However, how a calcium-dependent protein kinase (CPK) modulates this process remains elusive in rapeseed (*Brassica napus* L.). In the present study, we identified and characterized CPK6L from rapeseed as a novel regulator of ROS and cell death. The subcellular localization of BnaCPK6L was investigated through GFP and was found to be located at the endoplasmic reticulum membrane. Overexpression of the constitutively active BnaCPK6LCA resulted in significant accumulation of ROS and HR-like cell death than the full-length. A quantitative RT-PCR survey identified that the expression levels of a few ROS, cell death and defense-related marker genes were up-regulated upon *BnaCPK6LCA* expression. Mating-based split ubiquitin system (mbSUS) screening revealed that BnaCPK6L interacted with BnaRBOHD (Respiratory Burst Oxidase Homolog D), which was validated by bimolecular fluorescence complementation (BiFC). An *in vitro* phosphorylation assay indicated that BnaCPK6L phosphorylated BnaRBOHD. Lastly, we also found that three 2C type protein phosphatases (PP2Cs) interacted with BnaCPK6L. Taken together, this study indicates that BnaCPK6L plays an important role in ROS and HR-like cell death through interacting with and phosphorylating RBOHD.

1. Introduction

Reactive oxygen species (ROS) act as double-edged swords in plants. At low concentrations, they act as signal molecules to regulate growth, development and resistance to abiotic stresses; at high concentrations, ROS are toxic and damage many different cellular components [1]. Many different stressors can induce ROS accumulation [1]. Therefore, a tight control of ROS level is essential for trade-off between growth and stress or disease resistance. Plants have evolved an array of enzymes and non-enzymatic systems to produce or generate ROS [1]. Plasma membrane-localized respiratory burst oxidase homologs (RBOHs), homologs of mammalian NADPH oxidase (NOX), constitute a group of enzymes responsible for producing ROS [2]. It is reported that RBOHs play a pivotal role in both development and defense against pathogens [3]. Existing evidences demonstrate both transcription and post-translational phosphorylation play important roles in mediating the activities of RBOHs [4,5].

Ca^{2+} is a ubiquitous second messenger in eukaryotes. Calcium-dependent protein kinases (CPKs) constitute a family of Ser/Thr protein kinases broadly distributed in plants that decode Ca^{2+} signals [6]. CPKs consist of four domains, which are N-terminal variable domain (V), protein kinase domain (K), autoinhibitory junction domain (J) and C-terminal calmodulin-like domain (C) [7]. Past studies showed that the highly variable N-terminal domain may contain potential myristoylation or palmitoylation sites that are responsible for membrane association and substrate recognition [8,9]. Early studies also indicated that activations of plant CPKs relies on relief of autoinhibition [10,11].

CPKs are encoded by multigene families consisting of 34 members in Arabidopsis, and 31 in rice, which are clustered into four distinct subgroups [12,13]. Plant CPKs have been demonstrated to play important roles in many different physiological processes, including growth and development, hormone signalings, abiotic

* Corresponding author.
E-mail address: jiangyq@nwafu.edu.cn (Y.-Q. Jiang).

https://doi.org/10.1016/j.bbrc.2019.08.118
0006-291X/

and biotic stress tolerance [6,14,15]. For example, a few CPKs in Arabidopsis and rice have been found to positively or negatively regulate stress and disease tolerance by modulating ABA signaling and/or ROS levels [16–18].

Existing evidences show that CPKs can affect ROS levels through influencing the activities of RBOHs through phosphorylation in Arabidopsis and potato [4,8,19]. For example, StCDPK4 and StCDPK5 phosphorylate StRBOHB and regulate the oxidative burst [19]. AtCPK5 phosphorylates RBOHD and activates its activity [4]. Nevertheless, the substrates, functions and regulatory mechanisms of many CPKs in plants wait to be explored.

In contrast, protein phosphatases act as negative regulators of kinases-mediated signaling processes. In higher plants such as Arabidopsis, type 2C protein phosphatases (PP2Cs) constitute a large family with 76 members [20]. Among PP2Cs, clade A PP2Cs with nine members in Arabidopsis are reported to negatively regulate ABA signaling and stress responses [20]. AtCPK11 was found to interact with several members of clade A PP2Cs [21], suggesting that PP2Cs may antagonize CPKs. However, an investigation of interactions between clade A PP2Cs and ROS-related CPKs in plants has not been well established.

Rapeseed (*Brassica napus* L.) is an important oil crop in China and world-wide, providing editable oil and pasture to feed livestock. Previously, we systematically identified and cloned the cDNA sequences of a total of over 50 CPK and PP2C genes from rapeseed and performed a preliminary investigation [22]. Here, we studied the function and regulatory mechanism of BnaCPK6L.

2. Materials and methods

2.1. Plant materials and growth conditions

Rapeseed and *Nicotiana benthamiana* seeds were surface-sterilized and sown on 1/2 x MS medium for 7 d before transferred into a soil mix and grew in a growth chamber. The setting is a photoperiod of 14 h light/10 h dark with a light intensity of 120 μE m^{-2} s^{-1}, and a temperature of 22 °C and a relative humidity of 60–70%.

2.2. Phylogenetic tree construction and bioinformatics

The CPK sequences of representative plant species were retrieved from TAIR (www.arabidopsis.org) and NCBI databases. Multiple alignments of protein sequences were performed using ClustalX1.83. A phylogenetic tree was reconstructed using a maximum parsimony algorithm with MEGA6 software. The myristoylation and palmitoylation motifs were predicted by ExPaSy Myristoylator (http://web.expasy.org/myristoylator/) and CSS-Palm 3.0 (http://csspalm.biocuckoo.org/).

2.3. Subcellular localization and confocal microscopy

The coding region of *BnaCPK6L* was PCR-amplified and cloned into a binary vector of pYJGFP. After confirmation, the recombinant plasmid and P19 strain of tomato bushy stunt virus were introduced into the competent cells of *Agrobacterium tumefaciens* GV3101. Agroinfiltration into the leaves of 28-d-old *N. benthamiana* was performed as described previously [23]. Fluorescence signals were observed 2 d later on a TCS SP8 confocal microscope (Leica, Germany).

2.4. RT-PCR and quantitative RT-PCR (qRT-PCR)

Rapeseed seedlings of 7 d old were treated with 50 μM jasmonic acid (JA, Sigma, USA), 2 mM salicylic acid (SA, Sigma), 20 mM H_2O_2

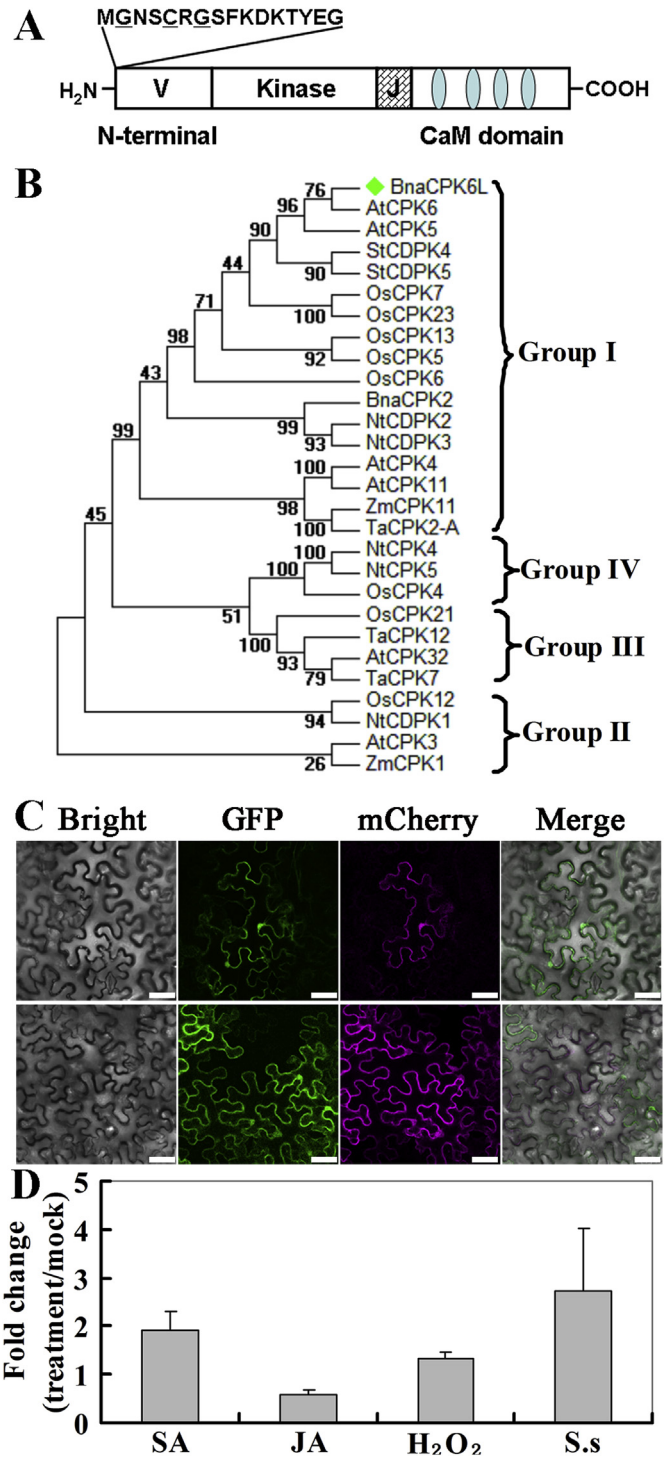

Fig. 1. Phylogenetic, subcellular localization and expression assays of BnaCPK6L. (A) A, Scheme of domain structure of BnaCPK6L. The N-terminal amino acid sequence is indicated at the top. A kinase catalytic domain is joined via a junction (J) domain to a calmodulin-like domain (CaM) with four calcium-binding motifs. (B) Phylogenetic relationship of BnaCPK6L with representative CPKs from various plants species. Percentages of bootstrapping of 1000 replicates are shown on the branches. (C) Subcellular localization of BnaCPK6L-GFP in *N.benthamiana*. *CBL1n-mCherry* (upper panel) and *CHS-mCherry* (lower panel) were co-expressed as the plasma and ER markers, respectively. The leftmost panel is bright field, the 2nd GFP field, the 3rd mCherry field, and the rightmost an overlay of the three images. Scale bar, 75 μm. (D) qRT-PCR assay of responses of *BnaCPK6L* to SA, JA, H_2O_2 and *S. sclerotiorum* treatments for 6 h. Values are means ± S.E. of three independent biological replicates.

(Alfa Aesar, France) and 18-d-old seedlings were inoculated with *S. sclerotiorum* or agar plug (control) as described previously [23]. Total RNA was extracted from leaves using Trizol (Sangon, China). After DNaseI treatment using the RapidOut DNA-free kit (Thermo Fisher Scientific), 2.5 μg RNA was used to synthesize cDNA using MMLV (RNase H-) reverse transcriptase and Oligo(dT)$_{18}$ primers (TaKaRa). PCR was performed with high-fidelity PrimeStar HS DNA polymerase (TaKaRa, Japan). cDNA samples for qRT-PCR were diluted ten times with sterile water and 2 μL of cDNA was used in qPCR using *SYBR* Green I premix (Baiao, China) on a CFX96 thermocycler (Bio-Rad, USA). *UP1* and *UBC9* of rapeseed and *L23* and *PP2A* of tobacco were used as reference genes and fold changes were calculated according to Ref. [22]. Three independent biological replicates were prepared and analyzed.

2.5. Site-directed mutagenesis

Site-directed mutagenesis PCR was performed via overlap PCR using high-fidelity *Pfu* DNA polymerase (Bioer, China) and the resulting plasmid was confirmed by sequencing. A total of six amino acid residues were mutated to construct BnaCPK6LCA and they are A361P/V362D/Q368P/F369E/S370D/A371L [8]. Primers are listed in Table S1.

2.6. Transient expression assay and physiological measurements

The CDS of *BnaCPK6L*, *BnaCPK6LCA* and *GFP* were cloned into a binary vector p35SFC and confirmed. Agroinfiltration into the lower epidermal side of 30 d old leaves of *N. benthamiana* plants were performed as described before [23]. Electrolyte leakage was measured according to Ref. [23]. Quantitative assays of malondialdehyde (MDA) was performed as previously described [24].

2.7. Mating-based split ubiquitin system (*mbSUS*) assay

BnaCPK6L CDS was cloned into pX-NubWTgate vector and transformed into the yeast strain THY.AP5. The CDSs of *BnaRBOHs* were cloned into pMetYCgate vector and transformed into the yeast strain THY.AP4. Diploid yeasts were selected on the selective SD medium. The titration assay was performed by growing yeast colonies on the synthetic minimal medium lacking leucine (L), tryptophan (W), histidine (H) and adenine hemisulfate (A) (SD-LWHA). β-galactosidase assay was performed as previously described [25].

2.8. Bimolecular fluorescence complementation (BiFC) assay

The CDS of respective genes were subcloned into 35S-SPYNE(R) 173 or 35S-SPYCE(M) vector [22]. Resulting plasmids were introduced into *A. tumefaciens* strain GV3101 cells, which were co-infiltrated together with the P19 strain into true leaves of 3-week-old *N. benthamiana*. YFP fluorescence was observed 3 d after infiltration on a confocal microscope (Leica, Germany).

2.9. Prokaryotic protein induction, purification and phosphorylation assay

Relevant genes (CDS) were subcloned into vector of pGEX-4T-1 (Amersham). Recombinant plasmids were transformed into BL21 (Codon Plus) strain of *E.coli* (Novagen), before induced by 0.5 mM isopropyl β-D-thiogalactoside (IPTG) for 8 h at 25 °C. Cell pellets were collected and then lysed by sonication in 1 × PBS. GST-tagged proteins were purified with GST-bind resin (Novagen) according to manufacturer's instructions.

Purified proteins were incubated in a kinase assay buffer (50 mM Hepes, pH 7.5, 10 mM $MgCl_2$, 2 mM DTT, 5 mM EGTA, 4.6 mM $CaCl_2$ and 50 μM ATP) in triplicate for 30 min at 25 °C. Then

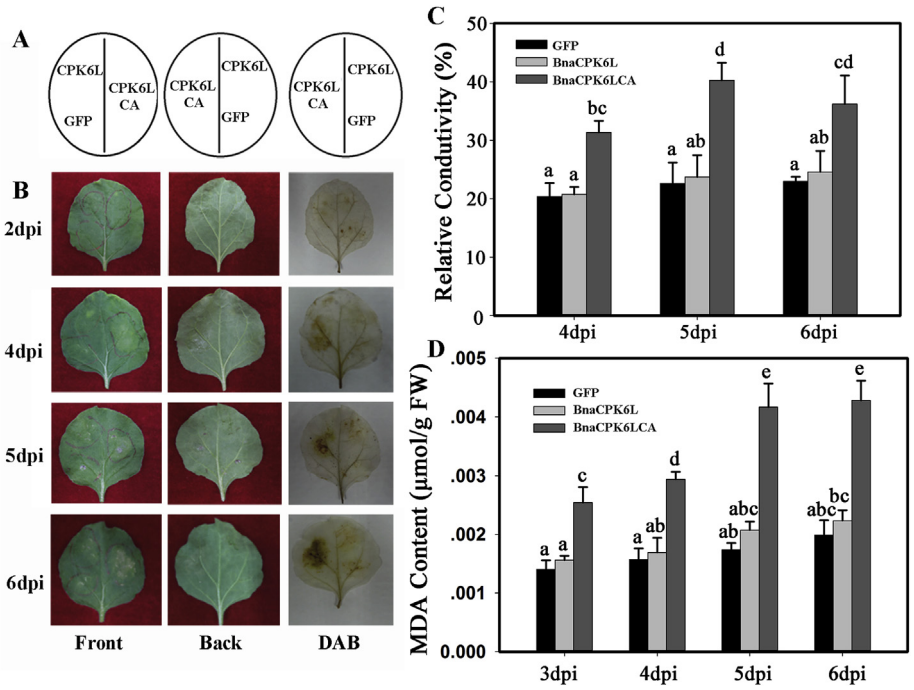

Fig. 2. Transient overexpression of constitutively active *BnaCPK6L* triggered ROS accumulation and HR-like cell death. (A) Scheme of sites of infiltrated samples in tobacco leaves. *GFP* was expressed as a control. (B) Photographs of tobacco leaves expressing *BnaCPK6L*, *BnaCPK6LCA* and *GFP* control at different days post-infiltration (dpi). The left, middle and right panels represent the front, back sides and DAB staining of accumulated ROS, respectively. (C–D) Quantification of relative conductivity and MDA contents in leaf tissues expressing *GFP*, *BnaCPK6L* or *BnaCPK6LCA* at different time points, respectively. Data are means of three independent assays± S.E. Identical and different lowercase letters represent non- and significant differences (P<0.05).

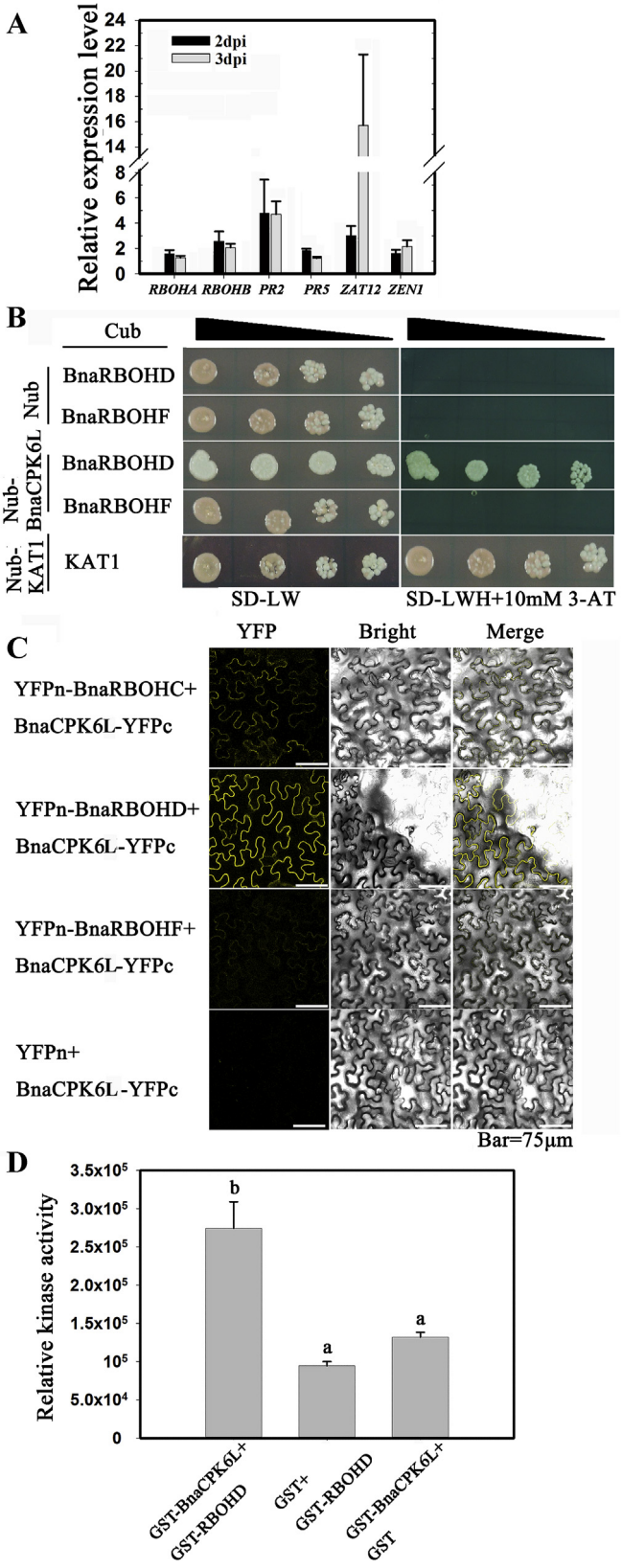

Fig. 3. Identification and validation of protein-protein interactions (PPI) between BnaCPK6L and BnaRBOHs. (A) qRT-PCR analysis of expression levels of ROS and defense-related marker genes. *GFP* (control) and *BnaCPK6LCA* were transiently expressed in tobacco leaves for 2 and 3 dpi before sampled. qRT-PCR was used to determine expression level of six marker genes. Data are means ± S.E. of three biological replicates. (B) Mating-based split ubiquitin system (mbSUS) examination of PPI. Yeast cells transformed with indicated plasmid combinations were grown on non-selective (SD-LW) and selective medium (SD-LWHA) media. Interaction between Arabidopsis K^+ channel 1(KAT1) and KAT1 was used as a positive control. 10-fold diluted yeast cell cultures are illustrated by black narrowing triangles. (C) Validation of PPI in tobacco leaves through bimolecular fluorescence complementation (BiFC) assay. The coding regions of *BnaCPK6L* and *BnaRBOHs* fused to the C- and N-terminal halves of YFP, respectively were co-expressed in leaf cells. The different plasmid combinations are indicated at the left side. The fluorescence of YFP was observed 3 d later on a confocal laser microscope. The left panel is YFP fluorescence, the middle bright field and the right an overlay of the two images. Scale bar, 75 μm. (D) *In vitro* kinase assay of BnaCPK6L phosphorylating BnaRBOHD. GST is used as the control for substrate. Data shown are the means ± SE of three independent replicates. Different letters indicate significant differences among reactions ($P < 0.05$).

an ADP-Glo kinase assay kit (Cat#V9101, Promega) was used to quantify ADP produced from kinase reactions following the manufacturer's manual. In brief, kinase reactions were stopped by adding ADP-Glo reagent and incubated for 1 h at 25 °C. Then, kinase detection reagent was added to each reaction tube and incubated for 1 h at 25 °C. Luminescence was recorded with a GloMax 20/20 luminometer (Promega).

2.10. Yeast two-hybrid (Y2H) assay

Y2H assay was performed using the MatchMaker yeast two-hybrid system (Clontech, USA). The coding regions of *BnaCPK6L* and *BnaPP2Cs* were subcloned into pGBKT7 (BD) and pGADT7 (AD) vectors, respectively. Recombinant plasmids were sequentially transformed into yeast strain AH109 competent cells as described in Yeast Protocols Handbook (Clontech). Transformed yeast cells were titrated on two sets of media, SD-Leucin-Tryptophan (SD-LW), SD-Leucin-Tryptophan-Histidine+2.5 mM 3′AT (SD-LWH+3-AT), and continued to grow at 30 °C for 2–7 d, followed by X-gal staining before photographed [22].

3. Results and discussion

3.1. Sequence, subcellular localization and expression assays of rapeseed CPK6L

BnaCPK6L, a homolog of *AtCPK6*, was cloned by RT-PCR from rapeseed seedlings. The coding region of *BnaCPK6L* is 1647 bp in length with the protein conceptually translated from its cDNA containing 548 amino acids. The molecular weight of BnaCPK6L is 61.5 kDa with an isoelectric point (pI) of 5.14. BnaCPK6L contains all the four canonical domains or motifs of CPKs (Fig. 1A). The N-terminal sequence of BnaCPK6L contains putative myristoylation and palmitoylation modification sites, which are Gly at site 2, Cys at site 5 and Gly at site 7 (Fig. 1A), which are supposed to be necessary and enough for association with membrane system [26]. A phylogenetic tree was inferred using amino acid sequences of representative CPKs. It can be seen that BnaCPK6L, together with CPKs from rice, tobacco, maize, and potato, belongs to Group I (Fig. 1B). To test the subcellular localization of BnaCPK6L, we fused it with GFP (Green Fluorescence Protein) and transiently expressed it in leaves of tobacco. In parallel, the N-terminal of CBL1 [27] and *Arabidopsis Chalcone Synthase* (*CHS*) gene fused with *mCherry* were co-expressed, which were used to indicate plasma and endoplasmic reticulum (ER), respectively. The results showed that BnaCPK6L-GFP was predominantly located to the ER membrane, and only a slight association with PM was observed (Fig. 1C).

Next, we investigated the responses of *BnaCPK6L* to SA, JA, H_2O_2 treatments and a fungal pathogen *Sclerotina sclerotiorum* challenge by qRT-PCR. The results revealed that expression of *BnaCPK6L* increased after SA, H_2O_2 and *S. sclerotiorum* treatments compared to mock treatments. However, JA treatment slightly down-

regulated the expression of *BnaCPK6L* (Fig. 1D).

3.2. Transient expression of BnaCPK6L triggers ROS accumulation and HR-like cell death

To explore the role of *BnaCPK6L*, we generated overexpression plasmids of it for expression in leaves of *N.benthamiana* plants under the control of cauliflower mosaic virus 35S (CaMV 35S) promoter. Moreover, the constitutively active form BnaCPK6LCA was constructed by substituting six amino acid residues in the junction domain with other amino acids, which is expected to act as a constitutively active kinase [8]. *GFP* in the same vector was used as a control (Fig. 2A). Overexpresion of *BnaCPK6LCA*, but not *BnaCPK6L* remarkably induced ROS production in tobacco leaves, which was reflected by a 3,3′-diaminobenzidine (DAB) staining. Moreover the sites of expressing *BnaCPK6LCA* showed evident HR-like cell death, decoloring and drying, compared to *BnaCPK6L* and *GFP* expression sites (Fig. 2B).

We further quantified and compared relative conductivities and malondialdehyde (MDA) contents. Consistent with expectation, the relative conductivity of *BnaCPK6LCA*-expessing leaf tissues was significantly higher than that of *BnaCPK6L* or *GFP*-expressing tissues (Fig. 2C). Similarly, the MDA content in leaf tissues expressing *BnaCPK6LCA* was significantly higher than that in *BnaCPK6L* or *GFP*-expression tissues (Fig. 2D).

3.3. Examination of transcript changes of six marker genes related to ROS production, cell death and defense response

To understand the underlying mechanism of BnaCPK6LCA-triggerred ROS production and cell death, we used qRT-PCR to examine the mRNA changes of six marker genes implicated in ROS production, cell death and defense response. Among those, RBOHA and RBOHB were previously reported to determine apoplasitc ROS production [28]. *Zinnia Endonuclease 1* (*ZEN1*) encoding a nuclease involved in PCD of apical bud meristem [29]. *ZAT12* codes for a C2H2-type zinc finger transcription factor regulating H_2O_2-induced gene expression [30]. *Pathogenesis-related (PR) 2* and *PR5* are two markers of HR to many pathogens [31]. The results demonstrated that all the six marker genes are up-regulated upon *BnaCPK6LCA* expression, though the amplitude was different at two time points assayed (Fig. 3A).

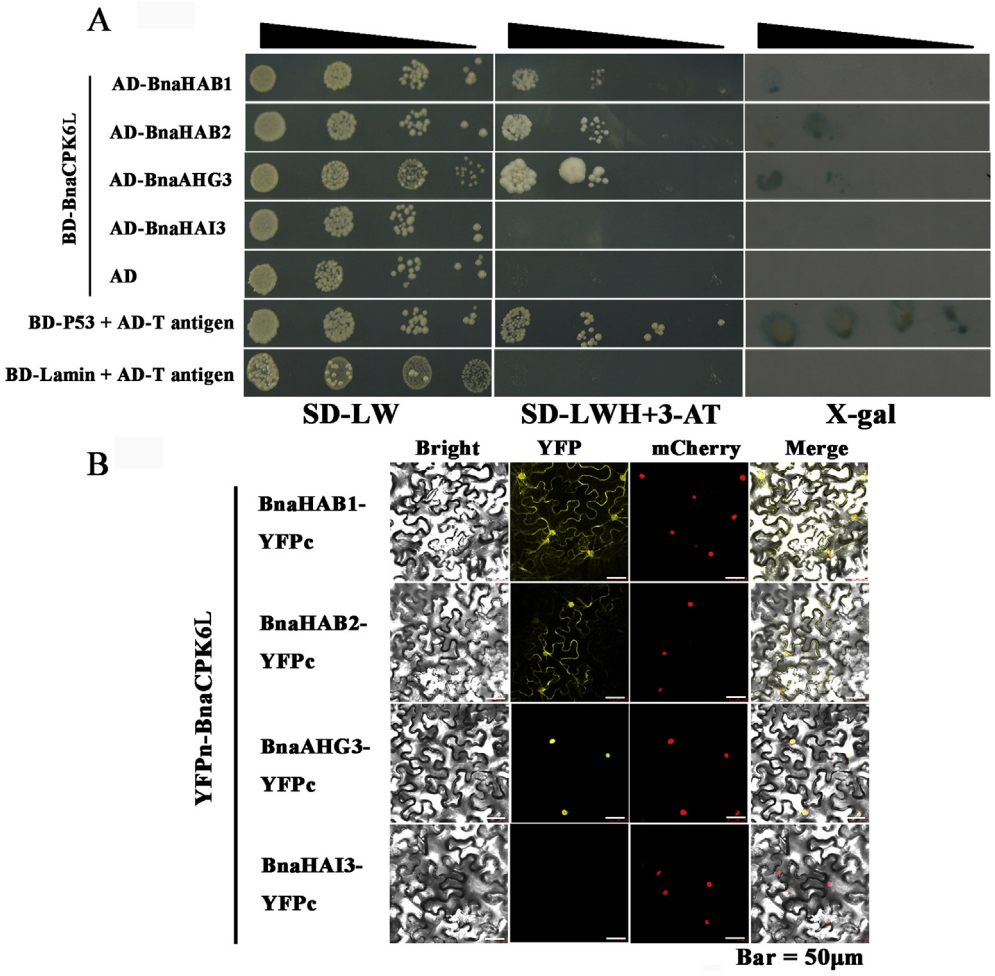

Fig. 4. Identification and validation of protein-protein interactions (PPI) between BnaCPK6L and BnaPP2Cs. (A) Yeast two-hybrid (Y2H)-based analysis of PPI. Yeast cells transformed with indicated plasmid combinations were grown on non-selective (SD-LW) and selective medium (SD-LWH+3-AT) media followed by β-galactosidase assay (X-Gal staining). Interaction between T antigen and P53 was used as a positive control, while that of lamin and T antigen as a negative control. 10-fold diluted yeast cell cultures are illustrated by black narrowing triangles. (B) Validation of PPI in tobacco leaves through BiFC assay. The coding regions of *BnaCPK6L* and *BnaPP2Cs* fused to the N- and C-terminal halves of YFP, respectively were co-expressed in leaf cells. The different plasmid combinations are indicated at the left side. The fluorescence of YFP was observed 3 d later on a confocal laser microscope. The left panel is bright field, the 2nd YFP, the 3rd NLS-mCherry and the rightmost an overlay of the three images. Scale bar, 50 μm.

3.4. Identification of interacting BnaRBOHs of BnaCPK6L

Two previous reports have shown that CPK from Arabidopsis and potato act as important regulators of RBOHs through phosphorylation [8,32]. We therefore were curious to know whether BnaCPK6L had a similar mechanism. To this end, we first used mbSUS technology to screen the putative substrates of BnaCPK6L, since RBOHs are well-known membrane proteins. Tobacco RBOHA and RBOHB are orthologs of RBOHF and RBOHD, respectively in Arabidopsis [28]. The results showed that BnaCPK6L interacted strongly with BnaRBOHD, but not with BnaRBOHF or other BnaRBOHs such as BnaRBOHC (data not shown); the positive control of KAT1 also showed an evident interaction with itself (Fig. 3B). Next, we validated the protein-protein interaction (PPI) by bimolecular fluorescence complementation (BiFC) technique. BnaCPK6L and BnaRBOH proteins fused to the C- or N-terminal half of YFP were co-expressed in tobacco leaves. The results showed that co-expression of *BnaRBOHD* and *BnaCPK6L* reconstructed YFP, whereas the other combinations including the empty YFPn vector control did not (Fig. 3C), which is consistent with the mbSUS result.

3.5. BnaCPK6L phosphorylates BnaRBOHD

To test whether BnaCPK6L can phosphorylate BnaRBOHD *in vitro*, we performed a luminescence-based kinase assay using proteins expressed and purified from *E.coli*. In this luminescence assay, the amount of ADP formed from ATP after phosphorylation was measured. GST expressed and purified in parallel was used as a control. The result showed that BnaCPK6L showed a significant phoshorylation activity towards BnaRBOHD, but not GST (Fig. 3D).

3.6. BnaCPK6L interacts with three BnaPP2Cs

To identify the antagonizing protein phosphatases that interact with BnaCPK6L, we used conventional yeast two-hybrid (Y2H) technique. Eight PP2Cs genes were cloned into pGADT7 vector containing the coding sequencing of activation domain (AD), while that of *BnaCPK6L* into pGBKT7 containing DNA-binding domain (BD). As shown in Fig. 4A, the positive and negative controls worked and BnaCPK6L interacted with BnaHAB1, BnaHAB2 and BnaAHG3, but not with any other BnaPP2Cs, indicating the specificity of PPI. We further validated the PPI in tobacco using BiFC. The results showed that BnaCPK6L interacted with BnaHAB1, BnaHAB2 and BnaAHG3 specifically, at different subcellular compartments. As a control, BnaCPK6L did not show any interaction with BnaHAI3 (Fig. 4B). The results of Y2H and BiFC are identical, supporting the usefulness of the two techniques in studying a BnaCPK.

In this study, we characterized rapeseed *BnaCPK6L* and found that BnaCPK6L positively regulated ROS production and cell death through interacting with and phosphorylating BnaRBOHD, but not BnaRBOHF. Further studies could be directed to decipher the roles of more BnaCPKs in ROS signaling and defense responses.

Conflicts of interest

The authors have no conflicts of interest to declare.

All third-party financial support for the work has been mentioned in the submitted manuscript.

Author contributions

Conceived and designed the experiments: YQJ and BY. Performed the experiments: GP, HZ and BC. Contributed materials: SG; Analyzed the data: GP and YQJ. Wrote the paper: YQJ.

Acknowledgements

This work is supported in part by the National Natural Science Foundation of China (No. 31471153), the Open Project [grant No. A314021402-1803] and the Natural Science Foundation of Shaanxi Province (2015JM3076). We thank Drs. Jörg Kudla (Universität Münster), Jia Li, Kai He (Lanzhou University) for providing the BiFC and mbSUS vectors, respectively. We also thank Dr. Jian-ye Chen (South China Agricultural University) for providing the yeast control plasmids.

Transparency document

Transparency document related to this article can be found online at https://doi.org/10.1016/j.bbrc.2019.08.118

Appendix A. Supplementary data

Supplementary data to this article can be found online at https://doi.org/10.1016/j.bbrc.2019.08.118.

References

[1] K. Apel, H. Hirt, Reactive oxygen species: metabolism, oxidative stress, and signal transduction, Annu. Rev. Plant Biol. 55 (2004) 373–399.
[2] M.A. Torres, J.L. Dangl, Functions of the respiratory burst oxidase in biotic interactions, abiotic stress and development, Curr. Opin. Plant Biol. 8 (2005) 397–403.
[3] M.A. Torres, J.L. Dangl, J.D. Jones, Arabidopsis gp91phox homologues AtrbohD and AtrbohF are required for accumulation of reactive oxygen intermediates in the plant defense response, Proc. Natl. Acad. Sci. U. S. A. 99 (2002) 517–522.
[4] U. Dubiella, H. Seybold, G. Durian, E. Komander, R. Lassig, C.P. Witte, W.X. Schulze, T. Romeis, Calcium-dependent protein kinase/NADPH oxidase activation circuit is required for rapid defense signal propagation, Proc. Natl. Acad. Sci. U. S. A. 110 (2013) 8744–8749.
[5] L. Yang, C. Ye, Y. Zhao, X. Cheng, Y. Wang, Y.Q. Jiang, B. Yang, An oilseed rape WRKY-type transcription factor regulates ROS accumulation and leaf senescence in Nicotiana benthamiana and Arabidopsis through modulating transcription of RbohD and RbohF, Planta 247 (2018) 1323–1338.
[6] J. Kudla, O. Batistic, K. Hashimoto, Calcium signals: the lead currency of plant information processing, Plant Cell 22 (2010) 541–563.
[7] A.C. Harmon, M. Gribskov, E. Gubrium, J.F. Harper, The CDPK superfamily of protein kinases, New Phytol. 151 (2001) 175–183.
[8] S. Asai, T. Ichikawa, H. Nomura, M. Kobayashi, Y. Kamiyoshihara, H. Mori, Y. Kadota, C. Zipfel, J.D. Jones, H. Yoshioka, The variable domain of a plant calcium-dependent protein kinase (CDPK) confers subcellular localization and substrate recognition for NADPH oxidase, J. Biol. Chem. 288 (2013) 14332–14340.
[9] T. Ito, M. Nakata, J. Fukazawa, S. Ishida, Y. Takahashi, Alteration of substrate specificity: the variable N-terminal domain of tobacco Ca(2+)-dependent protein kinase is important for substrate recognition, Plant Cell 22 (2010) 1592–1604.
[10] J.F. Harper, J.F. Huang, S.J. Lloyd, Genetic identification of an autoinhibitor in CDPK, a protein kinase with a calmodulin-like domain, Biochemistry 33 (1994) 7267–7277.
[11] B.C. Yoo, A.C. Harmon, Intramolecular binding contributes to the activation of CDPK, a protein kinase with a calmodulin-like domain, Biochemistry 35 (1996) 12029–12037.
[12] T. Asano, N. Tanaka, G. Yang, N. Hayashi, S. Komatsu, Genome-wide identification of the rice calcium-dependent protein kinase and its closely related kinase gene families: comprehensive analysis of the CDPKs gene family in rice, Plant Cell Physiol. 46 (2005) 356–366.
[13] S.H. Cheng, M.R. Willmann, H.C. Chen, J. Sheen, Calcium signaling through protein kinases. The Arabidopsis calcium-dependent protein kinase gene family, Plant Physiol. 129 (2002) 469–485.
[14] M. Boudsocq, J. Sheen, CDPKs in immune and stress signaling, Trends Plant Sci. 18 (2013) 30–40.
[15] A. Liese, T. Romeis, Biochemical regulation of in vivo function of plant calcium-dependent protein kinases (CDPK), Biochim. Biophys. Acta 1833 (2013) 1582–1589.
[16] T. Asano, N. Hayashi, S. Kikuchi, R. Ohsugi, CDPK-mediated abiotic stress signaling, Plant Signal. Behav. 7 (2012) 1–5.
[17] S. Campo, P. Baldrich, J. Messeguer, E. Lalanne, M. Coca, B. San Segundo, Overexpression of a calcium-dependent protein kinase confers salt and drought tolerance in rice by preventing membrane lipid peroxidation, Plant Physiol. 165 (2014) 688–704.
[18] S.Y. Zhu, X.C. Yu, X.J. Wang, R. Zhao, Y. Li, R.C. Fan, Y. Shang, S.Y. Du, X.F. Wang, F.Q. Wu, Y.H. Xu, X.Y. Zhang, D.P. Zhang, Two calcium-dependent protein

kinases, CPK4 and CPK11, regulate abscisic acid signal transduction in Arabidopsis, Plant Cell 19 (2007) 3019–3036.
[19] M. Kobayashi, I. Ohura, K. Kawakita, N. Yokota, M. Fujiwara, K. Shimamoto, N. Doke, H. Yoshioka, Calcium-dependent protein kinases regulate the production of reactive oxygen species by potato NADPH oxidase, Plant Cell 19 (2007) 1065–1080.
[20] A. Schweighofer, H. Hirt, I. Meskiene, Plant PP2C phosphatases: emerging functions in stress signaling, Trends Plant Sci. 9 (2004) 236–243.
[21] T. Lynch, B.J. Erickson, R.R. Finkelstein, Direct interactions of ABA-insensitive(ABI)-clade protein phosphatase(PP)2Cs with calcium-dependent protein kinases and ABA response element-binding bZIPs may contribute to turning off ABA response, Plant Mol. Biol. 80 (2012) 647–658.
[22] H. Zhang, W.Z. Liu, Y. Zhang, M. Deng, F. Niu, B. Yang, X. Wang, B. Wang, W. Liang, M.K. Deyholos, Y.Q. Jiang, Identification, expression and interaction analyses of calcium-dependent protein kinase (CPK) genes in canola (Brassica napus L.), BMC Genomics 15 (2014) 211.
[23] M.S. Rehmani, Q. Chen, J. Yan, X. Cui, S. Gao, F. Niu, L. Yang, B. Yang, Y.-Q. Jiang, A novel stress-responsive BnaNAL1 transcriptional activator in oilseed rape positively modulates reactive oxygen species production and cell death, Environ. Exp. Bot. 163 (2019) 1–14.
[24] F. Niu, B. Wang, F. Wu, J. Yan, L. Li, C. Wang, Y. Wang, B. Yang, Y.Q. Jiang, Canola (Brassica napus L.) NAC103 transcription factor gene is a novel player inducing reactive oxygen species accumulation and cell death in plants, Biochem. Biophys. Res. Commun. 454 (2014) 30–35.
[25] P. Obrdlik, M. El-Bakkoury, T. Hamacher, C. Cappellaro, C. Vilarino, C. Fleischer, H. Ellerbrok, R. Kamuzinzi, V. Ledent, D. Blaudez, D. Sanders, J.L. Revuelta, E. Boles, B. Andre, W.B. Frommer, K+ channel interactions detected by a genetic system optimized for systematic studies of membrane protein interactions, Proc. Natl. Acad. Sci. U. S. A. 101 (2004) 12242–12247.
[26] M.J. Nadolski, M.E. Linder, Protein lipidation, FEBS J. 274 (2007) 5202–5210.
[27] O. Batistic, R. Waadt, L. Steinhorst, K. Held, J. Kudla, CBL-mediated targeting of CIPKs facilitates the decoding of calcium signals emanating from distinct cellular stores, Plant J. 61 (2010) 211–222.
[28] H. Yoshioka, N. Numata, K. Nakajima, S. Katou, K. Kawakita, O. Rowland, J.D. Jones, N. Doke, Nicotiana benthamiana gp91phox homologs NbrbohA and NbrbohB participate in H2O2 accumulation and resistance to Phytophthora infestans, Plant Cell 15 (2003) 706–718.
[29] P. Teper-Bamnolker, Y. Buskila, Y. Lopesco, S. Ben-Dor, I. Saad, V. Holdengreber, E. Belausov, H. Zemach, N. Ori, A. Lers, D. Eshel, Release of apical dominance in potato tuber is accompanied by programmed cell death in the apical bud meristem, Plant Physiol. 158 (2012) 2053–2067.
[30] S. Davletova, K. Schlauch, J. Coutu, R. Mittler, The zinc-finger protein Zat12 plays a central role in reactive oxygen and abiotic stress signaling in Arabidopsis, Plant Physiol. 139 (2005) 847–856.
[31] A. Stintzi, T. Heitz, V. Prasad, S. Wiedemann-Merdinoglu, S. Kauffmann, P. Geoffroy, M. Legrand, B. Fritig, Plant 'pathogenesis-related' proteins and their role in defense against pathogens, Biochimie 75 (1993) 687–706.
[32] M. Boudsocq, M.R. Willmann, M. McCormack, H. Lee, L. Shan, P. He, J. Bush, S.H. Cheng, J. Sheen, Differential innate immune signalling via Ca(2+) sensor protein kinases, Nature 464 (2010) 418–422.